THE ARCHIVE OF MECHANICAL ENGINEERING

VOL. LIV 2007 Number 1

DOI: 10.24425/ame.2007.131545

Key words: hydrodynamics, gas dynamics, oil consumption, elastic contact, surface roughness, piston engines

ANDRZEJ WOLFF [*], *JANUSZ PIECHNA* [**]

NUMERICAL SIMULATION OF PISTON RING PACK OPERATION WITH REGARD TO RING TWIST EFFECTS

The motion of a ring pack on a thin film covering a cylinder liner has been analysed. In contrast to the previous papers [30], [31], which considered a primary hydrodynamic phenomena (including mixed lubrication), in the present paper an additional degree of freedom of a ring i.e. a twist motion is also taken into account. Equations describing the twist of rings are presented and used in simulation. The twist phenomena of a single ring have been analysed in the past [25]. In this paper, the twist effects of separate rings forming a ring pack are considered. In the pack configuration, the twist of the upstream ring strongly influences the operation of the downstream ring. The phenomenon commonly treated as secondary effect seems to be influencing the ring motion strongly. Differences between results obtained applying and neglecting ring twist motion are analysed and discussed.

Nomenclature

A_c – real area of contact per unit circumference,
E' – composite elastic modulus,
F_{WA} – friction force per unit circumference due to asperity contact,
F_{fri} – friction force per unit circumference due to viscous shear,
F_{h} – radial hydrodynamic force per unit circumference,
h – nominal oil film thickness,
$\bar{h}_T$ – average separation (gap between the ring face and cylinder liner),
p – pressure,
$\bar{p}$ – mean hydrodynamic pressure,
t – time,

[*] *Warsaw University of Technology, Faculty of Transport, ul. Koszykowa 75, 00-662 Warsaw, Poland; E-mail: wolff@it.pw.edu.pl*

[**] *Warsaw University of Technology, Institute of Aeronautics and Applied Mechanics; ul. Nowowiejska 24, 00-665 Warsaw, Poland; E-mail: jpie@meil.pw.edu.pl*

u – piston velocity / axial velocity of moving ring face,
W_A – radial force per unit circumference due to asperity contact,
x – spatial coordinate,
β – asperity radius of curvature,
η – asperity density,
ρ – density of lubricant,
μ – oil dynamic viscosity,
ϕ_s – shear flow factor,
ϕ_x – pressure flow factor,
δ_1, δ_2 – roughness amplitudes (asperity heights) of surfaces measured from their mean levels,
δ – composite (combined) roughness (asperity height): $\delta = \delta_1 + \delta_2$,
σ_1, σ_2 – standard deviations of asperity height distributions: δ_1, δ_2,
$\sigma = \sqrt{\sigma_1^2 + \sigma_2^2}$ – composite root-mean-square (RMS) roughness.

1. Instroduction

Piston rings are important part of most internal combustion engines. Commonly a set of piston rings is used to form a dynamic gas seal between the piston and cylinder wall. The sliding motion of the piston forms a thin oil film between the ring land and cylinder wall, which lubricates the sliding components. The hydrodynamic force generated by this thin oil film is opposed by a combination of the gas pressure acting on the back side of each ring and the ring stiffness. Due to the dynamic nature of these forces, each individual ring is periodically compressed and extended as the piston runs through its cycle. The problem of studying this interaction is further complicated by the high temperatures involved, as these result in low oil viscosity and subsequently very low oil film thickness. The oil film is typically thick enough to expect the existence of mixed lubrication, so this phenomenon should also be taken into account. Numerical simulation of these processes, which take place in a typical piston ring pack operation, is not only interesting, but very important from practical application.

While mechanical models of piston ring motion considering ring deformation, tilting, twisting or even vibration are normal in engine design, the fluid flow problems accompanying the piston ring operation are not commonly understood or used. Typically, the complicated mechanical models of ring motion are formulated using very primitive flow models to describe the unsteady hydrodynamic and gas dynamic ring load.

The probable reason for this is the complicated nature of the flow model required and the necessity of using numerical methods for a solution. The

main aim of this work is to model an oil flow in a lubricating gap between a ring land and a cylinder liner in conjunction with the gas flow through the labyrinth seal formed by a set of rings.

2. Present state of knowledge

In order to build new models and codes for analysis of the piston ring operation the authors have undertaken a multi-direction literature search. First, papers presenting gas flows in the cylinder-piston seal were analyzed. Secondly, papers concerning lubrication problems were investigated. Finally attention was focused on problems of modelling rough surface lubrication. Works concerning numerical methods of solution of partial differential equations describing lubrication problems have been also analyzed.

Many researchers have investigated and analyzed gas flow models [10], [11], [14], [16], [29], [30]. The best available model of the gas flow in cylinder-piston sealing is the model developed by Koszałka [12], [17]. The proposed model contains what is probably a complete set of leak sources taking into account the main cause of leaks, the ring gaps, including their changes due to variation of cylinder bore caused by wear and thermal expansion. The model also considers rapid changes of the blow-out due to axial ring movements in a piston ring groove caused by gas, friction and inertial forces.

Many investigators describe an oil flow in a gap between the ring land and cylinder liner which is also found in sliding bearing systems [4], [5], [7], [9], [11], [15], [18], [21], [24], [25], [28], [31].

Two basic papers of Patir and Cheng [18], [19] include the formulation of a fluid flow model between rough surfaces. These authors propose a modification to the Reynolds equation containing additional coefficients and terms correcting pressure distribution and flow rates caused by the surface roughness. Values of correction coefficients were presented and analyzed. This model, primarily formed for analysis of sliding bearings, has been accepted and is commonly used in piston ring operation analysis.

The problem of two-surface contact is a basic problem considered in many papers [1], [2], [3], [5], [8], [15], [21]. The most realistic and complete model of two rough surfaces was proposed by Greenwood and Tripp [6]. This paper presents a basic theory of interaction of randomly distributed asperities on contacting surfaces, defining relations between statistic roughness parameters and normal and tangential forces of interaction.

Ruddy, Dowson and Economou [24] have presented an interesting paper that describes a model of an oil ring with two lips. This model joins the mixed lubrication model of Patir and Cheng [18], [19] with the model of elastic

interaction of rough surfaces of Greenwood and Tripp [6]. The pressure distribution in an oil gap was calculated using Reynolds equation analytically integrated.

A similar combined model of the ring operation in the case of mixed lubrication can be found in the work by Gui and Liu [7]. They also used the sub-model of Patir and Cheng in conjunction with the sub-model of Greenwood and Trip, but only a general form of solution method was presented.

The same solution scheme was repeated by Yun, Chung, Chun and Lee [31]. The solution of the pressure distribution in an oil gap was obtained by the analytical integration of Reynolds equation.

Due to usefulness of the combined mixed lubrication model, this model was also used in the presented work.

A solution of the Reynolds equation can be obtained only if proper boundary conditions are defined and used. The problem of a proper boundary on the outlet side of the oil gap definition exists. The work of Richardson and Borman [24] contains an analysis of a possible range of boundary conditions. After an analysis of afore-mentioned paper, a combination of Sommerfeld and Reynold's conditions was chosen for use in this work.

A definition of wet area boundaries in the case of partial lubrication is a separate problem. Rangert [23], Dowson et al. [4] and Jeng [10] consider different methods of wet area definition. After analysis of the afore-mentioned papers, a new algorithm for wet area definition was developed and used.

3. Model and sub-models

3.1. Sub-model of rough ring land-cylinder liner lubrication

A typical piston ring pack contains three rings of different shape (one lip or two lips). For the motion analysis of each, a similar technique can be applied.

A model of the ring motion contains two main components. The first one defines the hydrodynamic forces generated in the gap filled by the oil, the second one describes the pressure distribution in the volumes formed between piston rings.

The model simulating the hydrodynamic forces takes into account an axial and radial velocity of the ring and a pressure difference across the ring. Generally, the process of the oil flow in the gap is described by the Reynolds equation. Due to the possibility of ring motion very close to the liner surface, it is necessary to consider also an influence of surface roughness. Due to the complicated, generally random structure of the interacting surfaces separated only by an oil film, an oil flow in such conditions is different from the flow in

a channel with totally flat surfaces. When the thickness of an oil film is less than four mean values of the surface roughness, it is necessary to consider a modified version of Reynolds equation including coefficients representing a deformation of the flow field due to surface roughness. The main parameter of the surface state is a combined mean value of the roughness including individual parameters of piston ring land surface and cylinder liner surface.

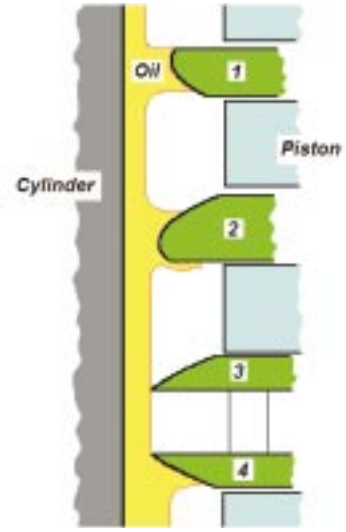

Fig. 1. Typical ring pack in an automotive engine

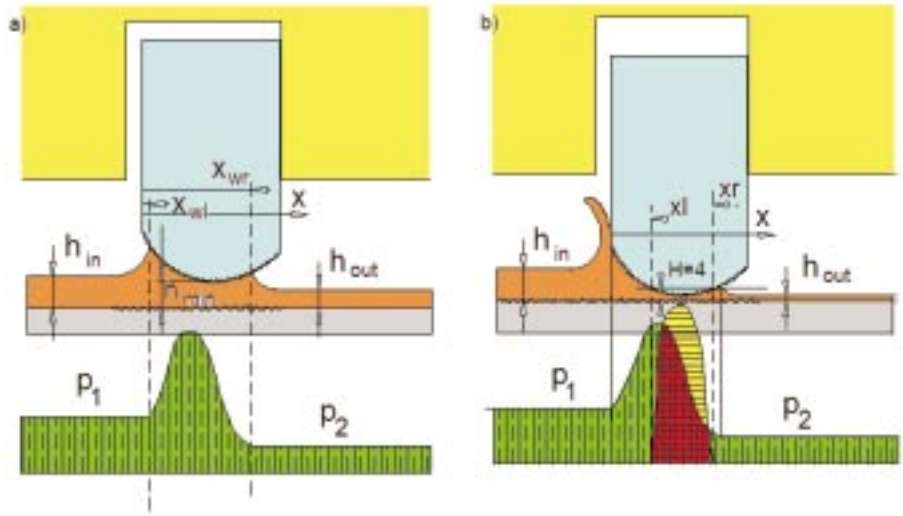

Fig. 2. Definition of geometrical parameters describing the flow phenomena in the case of full and mixed lubrication

The following form of modified Reynolds equation proposed by Patir and Cheng [19], [20] was used:

$$\frac{\partial}{\partial x}\left(\phi_x \frac{h^3}{12\mu}\frac{d\bar{p}}{dx}\right) = \frac{u}{2}\frac{d\bar{h}_T}{dx} + \frac{u}{2}\sigma\frac{d\phi_S}{dx} + \frac{d\bar{h}_T}{dt}. \tag{1}$$

The modified Reynolds equation includes additional coefficients and terms representing the flow transport due to the entrainment velocity and additional flow transport on account of the sliding action with a rough surface.

Particulars of application of that model in piston ring dynamic analysis can be found in the paper by Wolff and Piechna [31].

The model and parameters proposed by Patir and Cheng [19] were generally based on numerical simulation of the considered flow and were accepted and commonly used in the simulation of piston ring lubrication.

Additional coefficients used in the modified form of Reynolds equation tend to zero or one when the oil gap is sufficiently high. In this case, the modified Reynolds equation reaches the classical form for smooth surfaces.

Generally, the positive hydrodynamic force is generated in the convergent part of the ring land-liner gap. In the divergent part, the pressure drops down reaching cavitation level and commonly this area is ventilated to the back gas pressure.

Equation (1), after analytic or numerical integration, describes the pressure distribution in the ring and cylinder liner gap and after repeated integration defines the value and the line of action of the hydrodynamic force.

3.2. Sub-model of elastic contact between ring and liner

In the case of a very low gap height (less than 4 composite rms roughness σ) additional phenomena should be taken into account. At this range of oil film thickness, the possibility of a physical contact of highest elements (asperities) of rough interacting surfaces exists. Therefore, an elastic contact force had to be considered. This direct contact results in a piston ring and cylinder liner wear phenomena.

The commonly accepted and used model of contact of two rough surfaces was proposed and described by Greenwood and Tripp [6].

The normal contact force is described by the following relation [6]:

$$W_A = 16\sqrt{\frac{2}{15}}\pi\,(\eta\beta\sigma)^2\,E'\sqrt{\left(\frac{\sigma}{\beta}\right)}\int_{xl}^{xr} F_{5/2}\left(\frac{h}{\sigma}\right)dx. \tag{2}$$

The real contact area of interacting asperities is defined in the following way [6]:

$$A_c = \pi^2 (\eta\beta\sigma)^2 \int_{xl}^{xr} F_2\left(\frac{h}{\sigma}\right) dx \tag{3}$$

where integral boundaries $\boldsymbol{x_r}$ and $\boldsymbol{x_l}$ define the possible contact area $x_l \leq x \leq x_r$, in which the following relation is fulfilled $\frac{h}{\sigma} \leq 4$.
Components of the presented equations can be found in works by Greenwood and Tripp [6] and Wolff and Piechna [31].

3.3. Gas leakage sub-model

Depending on the aim of the simulation, different stages of simplification can be applied to modelling gas flows through piston seals. The simplest models consider the ring end gap as constant and the volume filled by gas between rings consisting of the sum of piston-cylinder gap, side ring-groove gap and back ring volume. Such a model is good enough to predict the pressure acting on the back side of the ring (Fig. 3, 4).

The model describing the leakage through the ring end gaps and defining the inter-ring pressure variation is based on the gas dynamic isentropic equations. It is assumed that the flow across the ring is realized mainly by the variable ring gap. The geometrical value of that gap is known, and the real flow conditions are defined by the contraction coefficient based on experimental data.

From measurements or numerical simulation of the pressure variation inside the cylinder during a full cycle, the pressure over the first sealing ring is known. The pressure between the first, second and third rings can be calculated assuming an isentropic process of expansion and compression in these volumes. Due to the relatively high pressure difference between these volumes, the gas dynamic equation including sonic and sub-sonic flows in orifices connecting volumes has been used. In the simplest model, it is assumed that gas leakage is limited only to the compensation gap between the ends of each ring.

Particulars of the flow model used can be found in papers by Wolff and Piechna [29], [30], [31], [32].

The inner gas energy inside each volume is taken as the difference between the energy delivered from the volume of higher gas pressure and energy transferred to the volume of lower gas pressure.

Taking into account the geometry and construction of the two-lip ring, it was assumed that no pressure difference exists across that type of ring.

More sophisticated models take into account variation of the ring end gap due to changes of the local cylinder bore due to thermal expansion.

In Fig. 11 exemplary pressure variation during one cycle of operation acting on the back side of rings are presented.

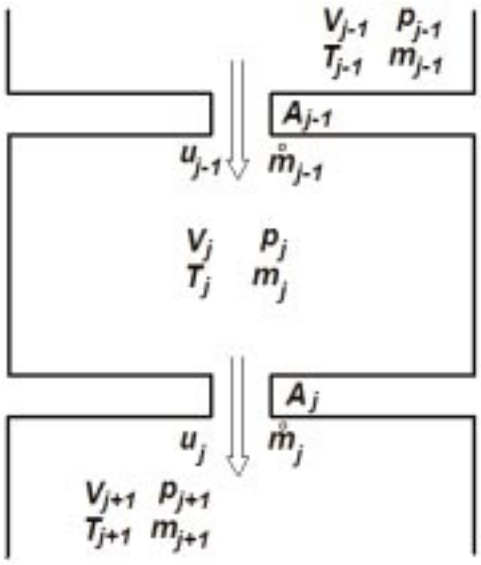

Fig. 3. Scheme of the gas flow though the ring compensation gap

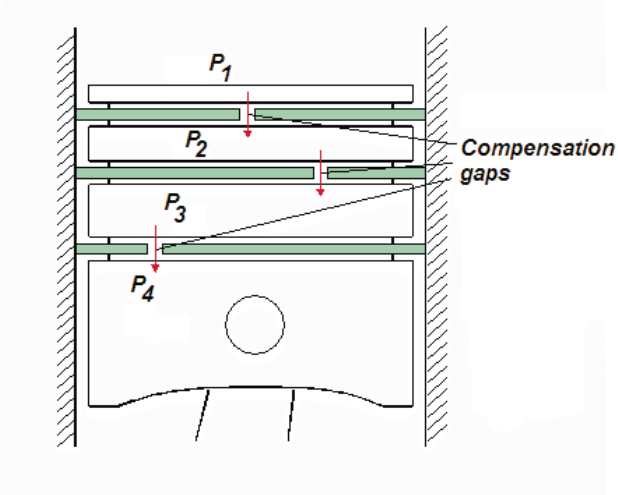

Fig. 4. Scheme of the gas flows through the ring sealing

3.4. Sub-model of ring equilibrium and ring twist

Due to the unavoidable clearance in piston grooves, the ring can elastically deform, twisting around the centre of gravity of the ring cross-section.

This generates changes in the gap geometry between the ring lip and cylinder liner. Radial and angular motion of the ring inside the groove causes surface wear and changes to the surface geometry of both the walls of the piston grooves and the side walls of the ring.

The absolute value of the angular ring elastic deformation (twist) seems to be very small. In many publications this effect is treated as a secondary effect, but assuming very small gap height, even very small changes in angular position of the gap wall can cause, in the scale of the gap, significant changes in local values of the gap height, resulting in great changes to the pressure distribution. Due to this fact, a sub-model of the ring twist has been prepared and combined with the existing model of the oil flow in the gap.

The presented study concentrates on the simulation of the ring twist process. The temporary radial position of the ring can be calculated by iteratively solving an equation of force equilibrium in the radial direction.

Hydrodynamic forces are totally compensated by the gas and ring stiffness forces. Due to the shift of the total hydrodynamic force in the direction of the leading side of the ring, a moment acting on the ring cross-section can be generated. Its value depends mainly on the shape of the ring surface.

Fig. 5 shows a scheme of forces acting on the rings, action lines and distances from the twist point for one and two lip ring types. Due to typical construction and the use of two lip rings, it was assumed that the gas pressure around the ring surfaces is the same. For this reason, gas forces were omitted in the scheme.

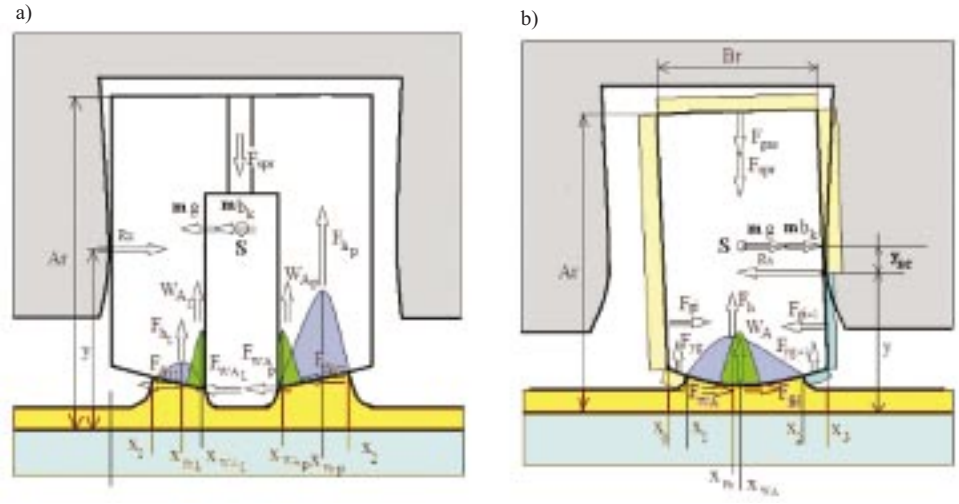

Fig. 5. Scheme and definitions of forces acting on piston rings with regard to twist angles: a) oil ring with two lips, b) compression or scraper ring as a single lip ring

Typical set of equations for a single lip ring has the following form:
a) in radial direction

$$\Sigma F_r = F_h + W_A + F_{yg_{i+1}} + F_{yg_i} - F_{spr} - F_{gas} = 0 \tag{4}$$

b) in axial direction

$$\Sigma F_x = R_x - F_{fri} - F_{cx} + F_{g_{i+1}} - F_{g_i} - \frac{m}{c_{imc}}(g + b_k) = 0 \tag{5}$$

Using these equations, we can calculate the reaction force between the ring and ring-groove in every time step. If the sign of this force changes, the axial movement of the ring in the ring-groove begins. At this point, the value of the reaction force $\boldsymbol{R_x = 0}$ and the axial movement of the ring relative to the piston groove can be described by the following differential equation:

$$\frac{m}{c_{imc}}\frac{d^2x_r}{dt^2} = -F_{fri} - F_{cx} + F_{g_{i+1}} - F_{g_i} - \frac{mg}{c_{imc}} \tag{6}$$

The ring movement is finished if the ring reaches the other side of the ring-groove.

If the possibility of ring twist is expected, this phenomenon complicates the solution because the radial force balance should be added to the momentum balance.

The ring twist has a strong influence on the shape of the gap and position of the transition point between the divergent and convergent part of the gap. The twist angle $\boldsymbol{\theta}$ of the first and second ring is mainly caused by the pressure forces acting on the side walls of the ring.

The twist around the centre of gravity of the ring cross-section (point S in Fig. 5b) can be described by the following equation:

$$\Sigma M_S = F_h(x_S - x_{F_h}) + W_A(x_S - x_{W_A}) - \left(F_{spr} + F_{gas}\right)\cdot 0 - \left(F_{fri} + F_{WA}\right)\cdot\frac{A_r}{2} + \\ + \left(F_{g_{i+1}} - F_{g_i}\right)\left(\frac{y}{2} + y_{sc}\right) + R_x \cdot y_{sc} + \frac{m}{c_{imc}}(g + b_k)\cdot 0 - K\cdot\theta = 0 \tag{7}$$

where:

F_h – hydrodynamic normal force
W_A – elastic direct rough surface contact normal force
F_{spr} – ring spring force
F_{gas} – back ring gas force
$F_{yg_{i+1}}$ – trailing edge gas force
F_{yg_i} – leading edge gas force

R_x – groove reaction force
F_{fri} – viscous friction force
F_{cx} – contact friction force
$F_{g_{i+1}}$ – trailing side gas force
F_{g_i} – leading side gas force
m – ring mass
g – gravitational acceleration
b_k – piston acceleration
c_{imc} – ring circumference.

If the torsional stiffness $\boldsymbol{K}$ of the ring is known, the ring twist angle $\boldsymbol{\theta}$ can be calculated.
The ring torsional stiffness $\boldsymbol{K}$ can be predicted by the following relation [27]:

$$K = \frac{E \cdot B_r^3 \cdot \ln\left(\frac{D}{d}\right)}{3\,(D+d)} \tag{8}$$

where:
E – ring material Young modulus,
B_r – ring height,
D – outer ring diameter,
d – inner ring diameter.

3.5. Sub-model of oil motion – calculation of wetted area

The ring lip surface area may be fully or partially wetted depending on the oil film thickness, axial ring velocity, gas pressure and ring stiffness. Expansion or contraction of the piston ring also has an influence on the wetted area of the ring land. Fully flooded lubrication is not a typical case, so a starved lubrication model has been developed and used.

The motion of each ring also transports the oil within the oil film. Some types of ring scrape and accumulate the oil in front of the ring. When the ring diameter is increased, some of the oil is pumped behind the ring. In the areas of starved oil flow, the thickness of the oil film becomes constant. In the presented model, the oil flow is carefully calculated.

Particulars of the model of wetted area boundaries developed by the authors can be found in the works by Wolff and Piechna [29], [30], [31], [32]. The algorithm is based on the control of the maximum pressure position. This point corresponds to the position of the linear velocity profile of oil in the gap. The radial motion of the ring changes the volume between the ring surface and cylinder liner, and some of the oil volume on the upstream gap part moves upstream and the rest downstream. Applying the mass conservation law, one can define the temporary position of the wet area boundaries.

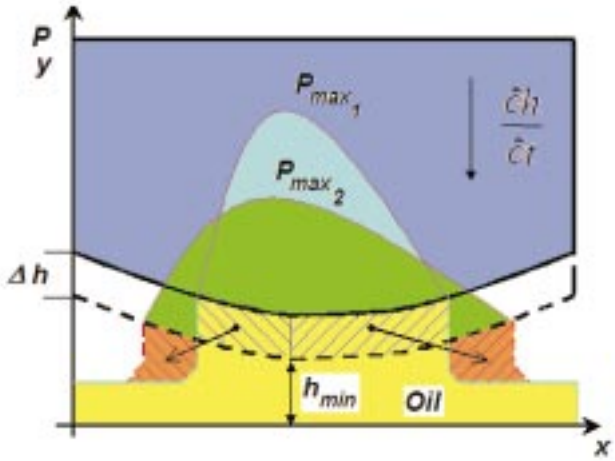

Fig. 6. Variation of the wetted area boundaries due to radial motion of the ring lip

In many models presented in literature, the authors do not take care of the oil scraped by the ring and assume that the oil is totally rejected and not used again. The authors of this paper used a model in which oil scraped by each ring is accumulated in front of the ring and redistributed again when the flow conditions change and oil can again be delivered to the gap.

In the case of higher oil temperature, mixed lubrication can be expected and interaction problems become more complicated. Now the wetted area can change and additionally, and independently, direct contact between interacting surfaces is possible.

4. Other effects

Many physical phenomena influencing piston ring operation can be treated as primary or secondary ones. The primary phenomena were considered in previous works by Wolff and Piechna [30], [31]. In this paper, some secondary phenomena have also been taken into account.

4.1. Temperature-dependent oil viscosity

Local temperature of the oil film can be assumed as equal to the cylinder liner temperature. Oil viscosity strongly depends on the temperature. Higher oil temperature means lower oil viscosity. Viscosity has direct influence on the hydrodynamic force generated in the ring – liner gap. The decrease of viscosity results in reduction of hydrodynamic load but not necessarily the friction force. Because the ring stiffness force and gas force are almost temperature independent, the reduction of oil viscosity results in lower oil film thickness during the sliding motion, which compensates the loss of

the hydrodynamic force caused by lower viscosity. The hydrodynamic force would remain constant, but is realized on a thinner oil film. In this way, viscosity influences the hydrodynamic force linearly and the size of the ring gap is included in Reynolds equation in the third power.

Whatever form the influence of oil temperature takes, the influence of temperature variation along the cylinder length is very interesting. Comparison of the oil film thickness on the cylinder liner for constant temperature (160°C) and linearly varying temperature (from 120°C at the crankshaft side to 200°C on the combustion chamber) is presented in Fig. 7. The remaining oil film thickness seems to be a good integral parameter defining the characteristics of ring motion.

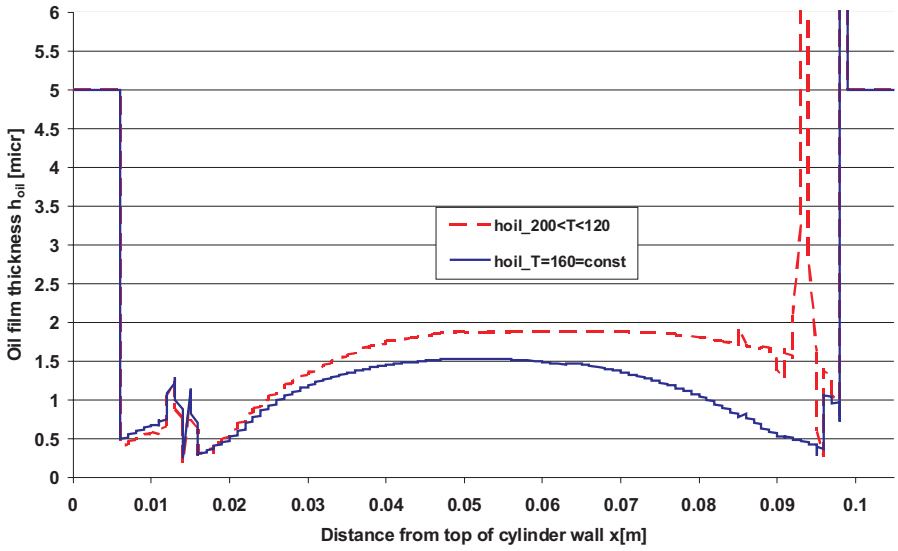

Fig. 7. Distribution of the oil film for constant oil temperature $\mathbf{h_{ref}}$ (160°C) and $\mathbf{h_{Tvar}}$ variable (from 200°C – left to 120°C – right). Calculation includes effects of rough surfaces and twisting movement of the rings

The increase of the oil film thickness in areas of lower oil temperature is visible. The definition of realistic temperature values along the cylinder length is a key element of the ring operation simulation.

4.2. Pressure-dependent oil viscosity

Viscosity of the oil is slightly influenced by the local pressure value. An increase in pressure also increases oil viscosity. In the range of pressures expected during engine operation, the increase of oil viscosity does not reach 25% of the oil viscosity value under atmospheric pressure. It seems that the influence of the pressure on the oil viscosity can be totally neglected.

4.3. Shear stress-dependent oil viscosity

Modern oils exhibit non-Newtonian features. Oil viscosity is slightly dependent on the local value of the oil shear stress. This phenomenon could be only important in the case of low oil viscosity which is accompanied by low gap sizes, increasing the shear stress values. The authors have made a number of numerical calculations and have proved that this can be treated as a secondary effect, only weakly influencing the piston operation.

5. Results of calculations including ring twist phenomena effects

For the analysis of the ring pack operation, a ring pack consisting of a single one-lip sealing (compression) ring, single one-lip scraping ring and a single two-lip scraping ring typically used in spark ignition engines of middle class automobiles has been selected.

The shape of the ring surface geometry is defined by a radius and offset of the maximum diameter of the ring outer surface in relation to the symmetry line of the ring, as shown in Fig. 8.

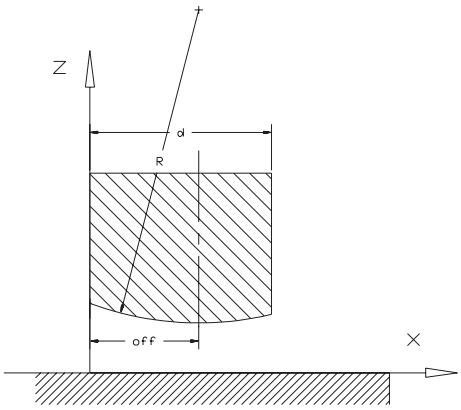

Fig. 8. Definition of the ring lip geometry

Basic geometrical parameters of the analyzed rings are collected in Table 1. Ring deformation geometry (vertical dimensions are 1000 times greater than horizontal ones) is depicted in Fig. 9. Ring surface roughness data and ring material properties are included in Table 2.

A linear temperature distribution of the cylinder wall from 120°C to 200°C has been assumed. The temperature variation results in differences in local oil viscosity values.

Table 1.

Input data of the ring pack

Ring 1:	
Ring width	B_1 = 1.48 mm
Offset of the ring profile	O_{ff1} = 0.37 mm
Surface radius	R_1 = 180 mm
Area of the ring compensation gap (gas flow)	A_1 = 0.014 mm^2
Ring elastic tension force (per unit circumference)	F_{SP1} = 375 N/m
Ring 2:	
Ring width	B_2 = 1.98 mm
Offset of the ring profile	O_{ff2} = 1.43 mm
Surface radius	R_2 = 180 mm
Area of the ring compensation gap (gas flow)	A_2 = 0.012 mm^2
Ring elastic tension force (per unit circumference)	F_{SP2} = 350 N/m
Ring 3 (with 2 lands):	
Total ring width	B_3 = 4.00 mm
Width of the upper ring land	B_{U3} = 1 mm
Width of the lower ring land	B_{L3} = 1 mm
Offset of the ring profile	O_{ff3} = 2 mm
Surface radius	R_3 = 244 mm
Area of the ring compensation gap (gas flow)	A_3 = 0.012 mm^2
Ring elastic tension force and spring force (per unit circumference)	F_{SP3} = 1545 N/m
Main engine parameters:	
Cylinder diameter	D_C = 80 mm
Piston diameter	D_P = 79.92 mm
Piston stroke	S = 79.5 mm
Length of connecting rod	l = 160 mm
Engine rotational speed	n = 3400 obr/min
Lubrication parameters:	
Growth velocity of the oil film thickness due to oil fog condensation on the cylinder liner under the ring pack	V_{fog} = 800 μm/s
Decrease velocity of the oil film thickness in combustion chamber due to evaporation	V_{evap} = 10 μm/s
Oil density	ρ = 900 kg/m^3

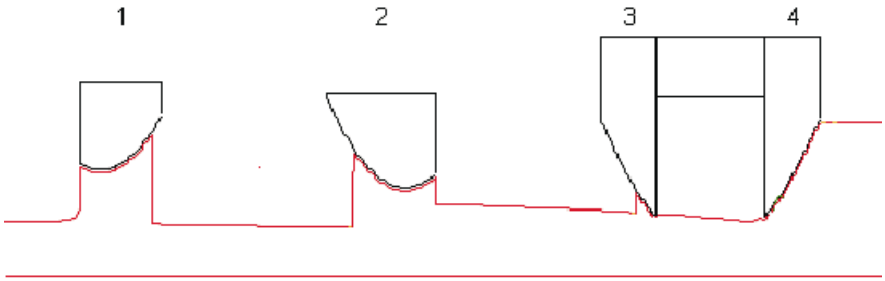

Fig. 9. Ring pack geometry under consideration (1 – compression ring, 2 – scraper ring, 3 – upper lip of the oil ring and 4 – lower lip of the oil ring); the continuous line represents the hypothetical oil film surface

Table 2.

Input parameters for surface roughness

Surface data	Value
Asperity density	$\eta = 1.114 \cdot 10^{12}$ [m^{-2}]
Asperity radius of curvature	$\beta = 0.2$ [μm]
RMS roughness of cylinder surface	$\sigma_1 = 0.22$ [μm]
RMS roughness of rings surface	$\sigma_2 = 0.044$ [μm]
Elastic modulus of cylinder liner	$E_1 = 1.13 \cdot 10^{11}$ [N/m^2]
Elastic modulus of rings	$E_2 = 1.5 \cdot 10^{11}$ [N/m^2]
Poisson's ratio of cylinder liner	$\nu_{P1} = 0.26$
Poisson's ratio of rings	$\nu_{P2} = 0.25$

A ring pack identical to that described above has previously been used in simulations which did not include the effects of ring twist. The main aim of that activity was collection of basic information about the behaviour of the rings with another step of freedom. The angle of ring twist was limited to angles confined by the ring and groove geometry.

Twist phenomena of single rings have been analyzed in the past [25]. Here, the twist phenomenon of separate rings forming a ring pack is considered. In the pack configuration, however, twist of the upstream ring always strongly influences the operation of the downstream ring.

Comparison of the oil film thickness distributions for twisting rings and not twisting rings is presented in Fig. 10. Significant reduction of the oil thickness in the case of twisting rings is clearly visible. It is seen mainly in the part of the cylinder cycle where the piston is closest to the cylinder head.

For the prospective engine designer and engine user, information about the oil thickness distribution generated by the moving ring pack is of the utmost importance. An exemplary one, calculated distribution of the oil film

thickness, is presented in Fig. 10. One can notice oil accumulated in spaces between rings. The right hand side of the figure corresponds to the crankshaft side and as a result the oil film is thicker on this side. Very low oil film thickness area corresponds to the top reversal point, where the gas pressure strongly loads the ring and the hydrodynamic effect of the oil film is reduced by the small linear ring velocity. Local increments of the oil thickness due to oil accumulation during ring motion in one direction, and oil release during motion in the opposite direction can be also observed. The most important is the very low thickness of the oil film near the top reversal point. Oil film thickness is in the range of $0.3 \div 0.4$ μm corresponding to the mean surface roughness values of the interacting surfaces of the ring and cylinder liner, equal to 0.22 μm. One can notice the relatively significant influence of the ring twist on the oil film thickness.

Typically, the figures presented below show the variation of some ring parameters as a function of the crankshaft rotation angle, beginning from the compression phase of the cylinder operation (0°).

Independently, pressure variations in the cylinder and in spaces between rings have been calculated and visualized in Fig. 11 for one full cycle of engine operation. Gas occupying spaces in the ring back (inner) surfaces forms the ring load, which tends to move the ring in the cylinder liner direction and reduces the oil film thickness. Very high values of pressure acting on the first sealing type ring in the pack (Fig. 11) are typical for this case.

Variation of the hydrodynamic forces acting against the gas and ring stiffness forces are presented in Fig. 12. Force values are calculated per unit of cylinder circumference.

Analyzing the data, one realizes that the gas force loading the sealing (compression) ring is 15 times greater than the ring stiffness forces. In the case of the one-lip scraper ring, the hydrodynamic force is up to 7 times greater than the ring stiffness force. The last (oil) two-lip ring has the slits between lips equalizing the pressure and, due to alternating operation using only one lip, is not pressure loaded. The last ring is loaded only by the ring stiffness force. As a result, it is necessary to generate a sufficiently high ring stiffness force and use very narrow ring lips.

In addition to forces generated by ring elasticity, gas pressure and hydrodynamic processes, the existence of additional contact forces in areas of mixed lubrication is expected. A reduction of hydrodynamic forces is compensated by the ring surface and cylinder liner contact forces. In Fig. 13 variation of the normal contact force components are presented for each ring. One can notice that maximal values of contact forces exist near the

piston turning points and are 3–4 times lower than the hydrodynamic forces in value.

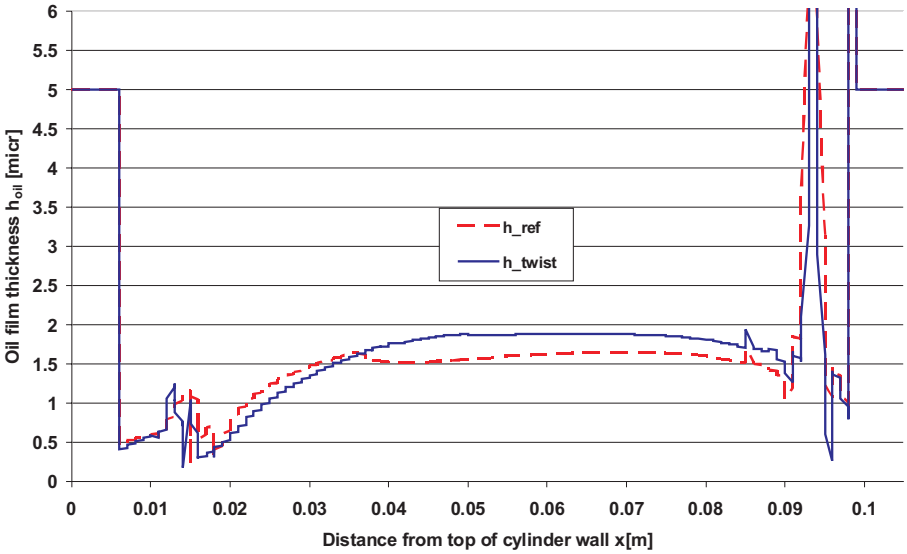

Fig. 10. Comparison of oil film thicknesses $\mathbf{h}_{\mathbf{ref}}$ and $\mathbf{h}_{\mathbf{twist}}$ left by the ring pack on cylinder liner ($\mathbf{h}_{\mathbf{ref}}$ – neglecting twist angles of piston rings, $\mathbf{h}_{\mathbf{twist}}$ – with regard to twist angles of rings)

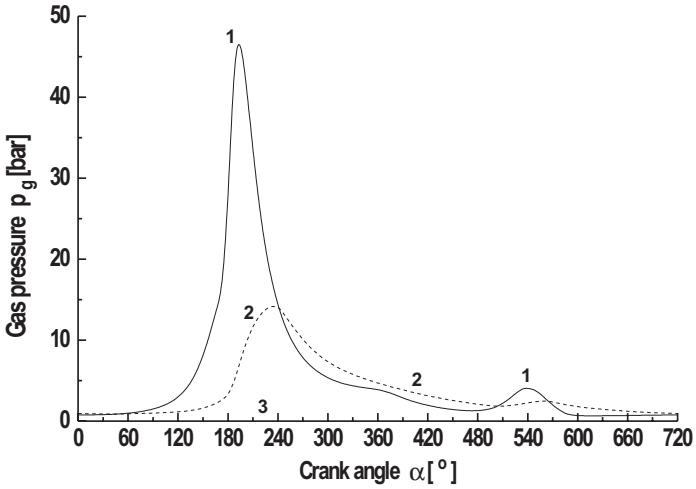

Fig. 11. Variation of the gas pressure acting on piston rings as a function of crankshaft rotation (1 – compression ring, 2 – scraper ring, 3 – oil ring)

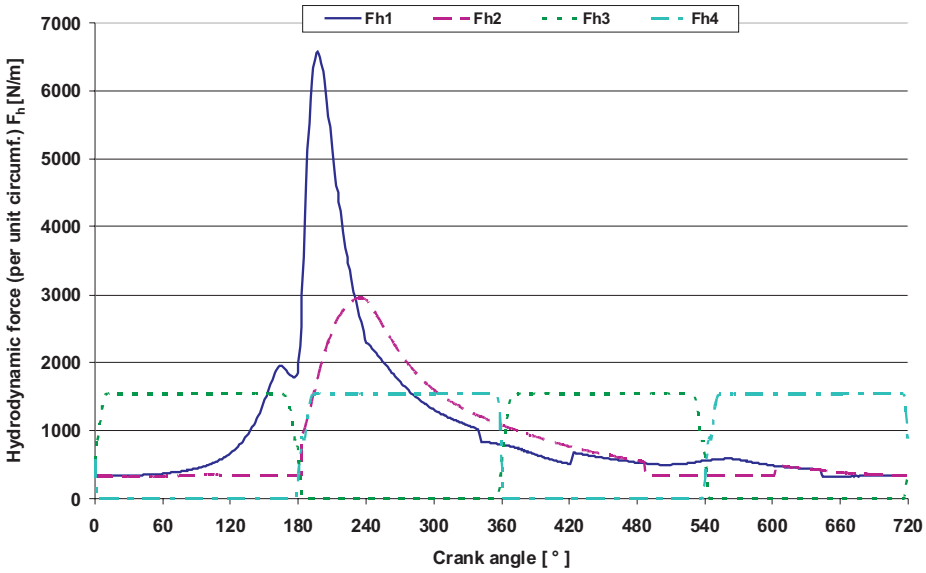

Fig. 12. Variation of hydrodynamic forces generated by each piston ring as a function of crankshaft rotation (1 – compression ring, 2 – scraper ring, 3 – upper lip of the oil ring and 4 – lower lip of the oil ring). Calculation results are for rough surfaces with linear variation of cylinder liner temperature (120–200°C) and no twist

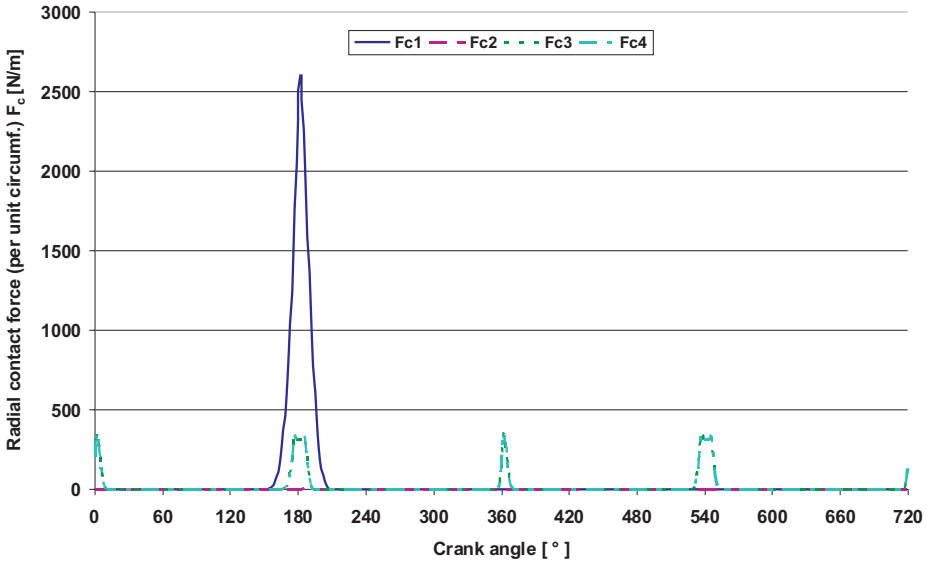

Fig. 13. Variation of radial components of contact forces for each piston ring as a function of crankshaft rotation (1 – compression ring, 2 – scraper ring, 3 – upper lip of the oil ring and 4 – lower lip of the oil ring). Calculation results are for rough surfaces with linear variation of cylinder liner temperature (120–200°C) and no twist

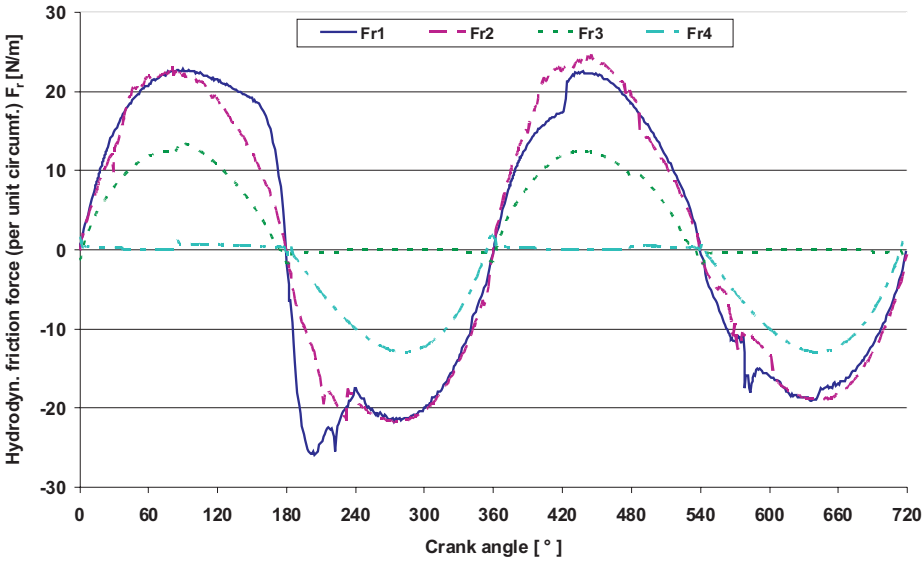

Fig. 14. Variation of hydrodynamic friction forces acting on each piston ring as a function of crankshaft rotation (1 – compression ring, 2 – scraper ring, 3 – upper lip of the oil ring and 4 – lower lip of the oil ring). Calculation results are for rough surfaces with linear variation of cylinder liner temperature (120–200°C) and no twist

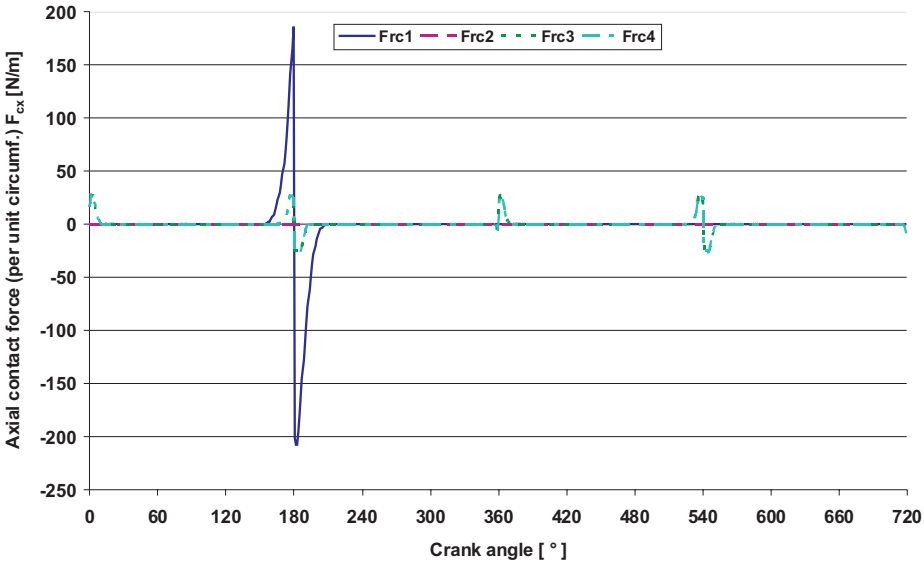

Fig. 15. Variation of tangential components of contact forces for each piston ring as a function of crankshaft rotation (1 – compression ring, 2 – scraper ring, 3 – upper lip of the oil ring and 4 – lower lip of the oil ring). Calculation results are for rough surfaces with linear variation of cylinder liner temperature (120–200°C) and no twist

Tangential hydrodynamic force variations for each ring in the pack, calculated during one cycle of engine operation, are shown in Fig. 14. It is clear that the tangential component of hydrodynamic forces generally depends on ring translational velocity and local variations are caused by the temporary ring radial motion and oil film thickness.

In Fig. 15 the tangential components of contact forces are presented. Such forces exist only near the piston turning points in phases of operation corresponding to the presence of highest cylinder pressure values (compression and work phase).

Variation of the minimum distance between the ring and cylinder wall as a function of crankshaft rotation angle is depicted in Fig. 16, 17, 18 for each ring. One can notice that phases of increased separation distance correspond to the highest values of translational piston velocity and that phases of very small separation exist near the piston turning point. After careful analysis, it can be seen that reduced separation distance is caused by the oil gathered by the preceding ring, resulting in lower oil film thickness. The separating oil film exists even in piston turning points.

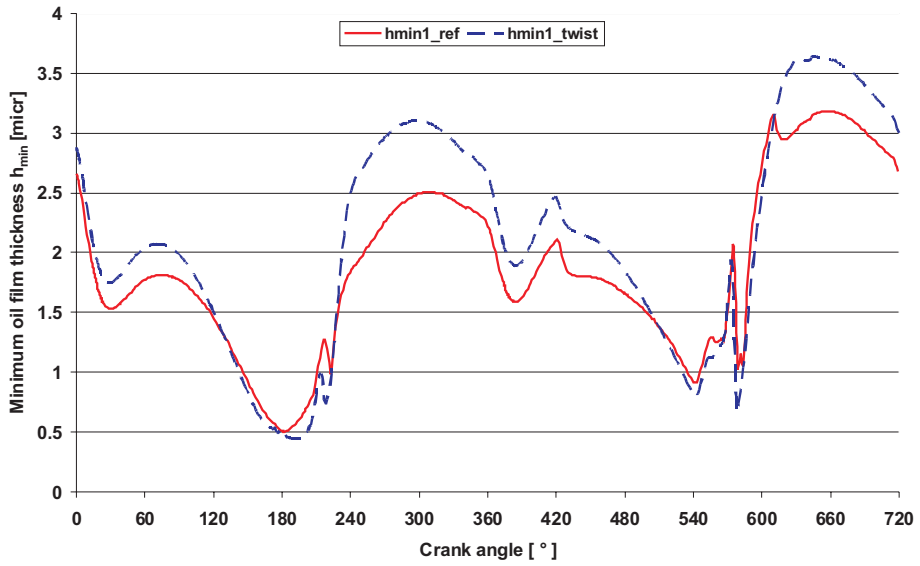

Fig. 16. Comparison of ring land-liner distances $\mathbf{h_{min1\_ref}}$ and $\mathbf{h_{min1\_twist}}$ for the compression ring ($\mathbf{h_{min1\_ref}}$ – disregarding twist angles of piston rings, $\mathbf{h_{min1\_twist}}$ – with consideration of twist angles of rings)

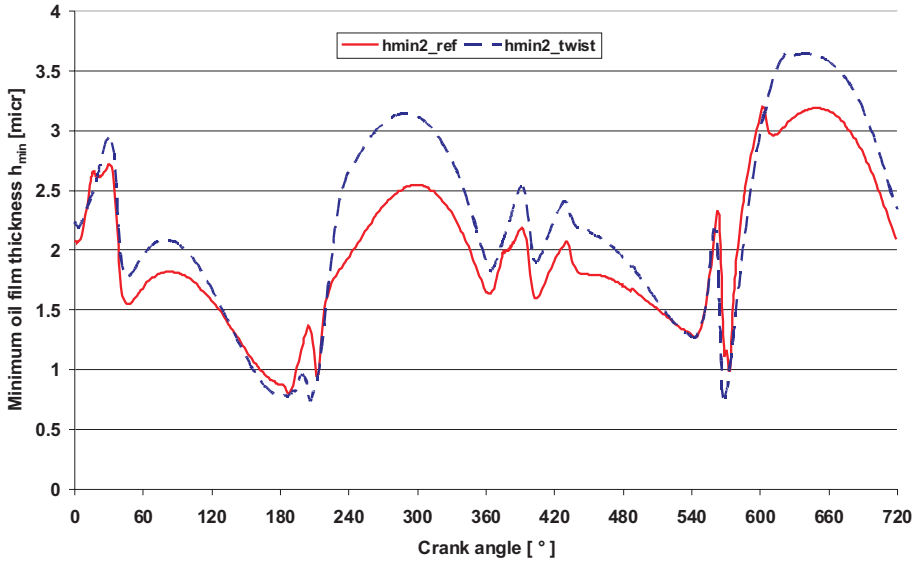

Fig. 17. Comparison of ring land-liner distances $\mathbf{h}_{\mathbf{min2\_ref}}$ and $\mathbf{h}_{\mathbf{min2\_twist}}$ for the scraper ring ($\mathbf{h}_{\mathbf{min2\_ref}}$ – disregarding twist angles of piston rings, $\mathbf{h}_{\mathbf{min2\_twist}}$ – with consideration of twist angles of rings)

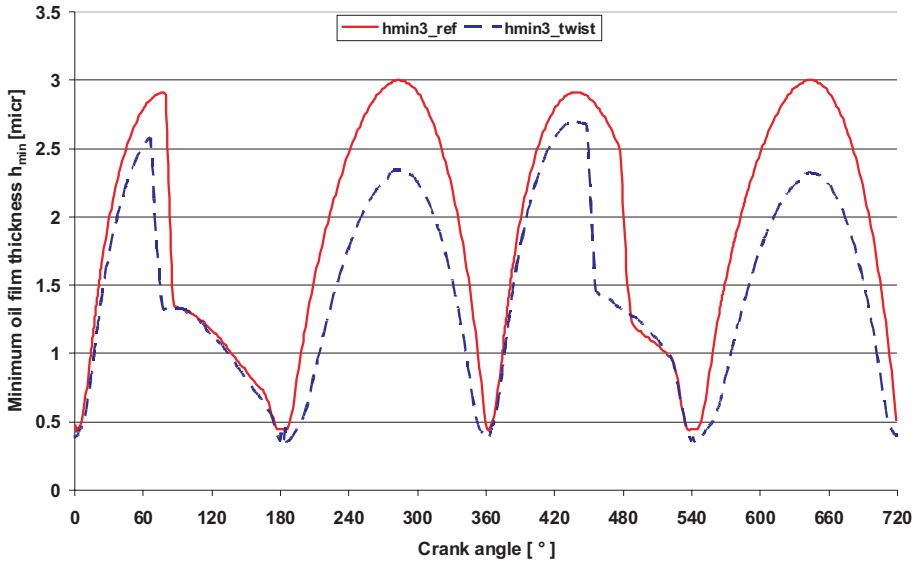

Fig. 18. Comparison of ring land-liner distances $\mathbf{h}_{\mathbf{min3\_ref}}$ and $\mathbf{h}_{\mathbf{min3\_twist}}$ for the oil ring ($\mathbf{h}_{\mathbf{min3\_ref}}$ – disregarding twist angles of piston rings, $\mathbf{h}_{\mathbf{min3\_twist}}$ – with consideration of twist angles of rings)

By comparing cycle phases applying to the same piston position but different gas pressures in cylinder, one finds that the first sealing (compression) ring is separated from the cylinder wall by only very thin oil film in phases of high gas pressure (see Fig. 16). Comparison of the minimal ring – cylinder liner gap of the compression ring shows rather significant differences in motion of the twisting ring in comparison with the steady one (Fig. 16).

Similar tendencies can be observed in the case of the second (scraper) ring (see Fig. 17). In this case, the gas pressure values are considerably lower due to the sealing action of the first ring. In the case of the third (oil) ring, the influence of the gas pressure on the ring – cylinder wall separation distance is not important and not taken into account (see Fig. 18). It can be seen that the average increase of the minimal distance between the ring and cylinder wall for first single-lip rings is contrary to the average decrease of this parameter in the case of the two-lip oil ring, resulting from the increase in scraped oil volume.

Detailed information about the oil accumulated by particular ring lips is collected in Figs. 19, 20, 21, 22, 23. It can be seen that high oil accumulation is characteristic of the oil ring operation, especially during the downstroke ($180 \div 360^\circ$ and $540 \div 720^\circ$). During the reversing motion, cylinder walls are exposed to oil fog penetration and the growth of the oil film thickness is observed.

The quantities of oil scraped by the compression and scraper rings are different. This is the result of different profiles of the ring contact surfaces (see Fig. 9). Compression rings accumulate oil during upward direction of motion and scraper rings during the opposite motion direction. One can see an influence of the ring twist on the scraping function of rings. It is a particularly strong effect in the case of accumulation of oil in the gap between lips of the oil ring.

One important computational problem is the definition of the boundaries $\boldsymbol{x_1}$, $\boldsymbol{x_2}$ of the ring wetted area (see Fig. 6). After a series of piston operation cycles, each ring scrapes and accumulates excessive oil, leaving behind an oil film not sufficient for full lubrication. Variation of the wetted area has an essential influence on the hydrodynamic bearing force of the ring and the resulting radial ring velocity.

Oil film thickness, piston velocity, ring stiffness and ring surface roughness parameters have significant influence on changes of wetted area boundaries and areas of direct contact of the ring and cylinder liner surfaces in the case of mixed lubrication.

Most often rings are only partially wetted in phases of high piston velocity. Rings are fully wetted in the piston motion phases corresponding to low velocity near the reverse points.

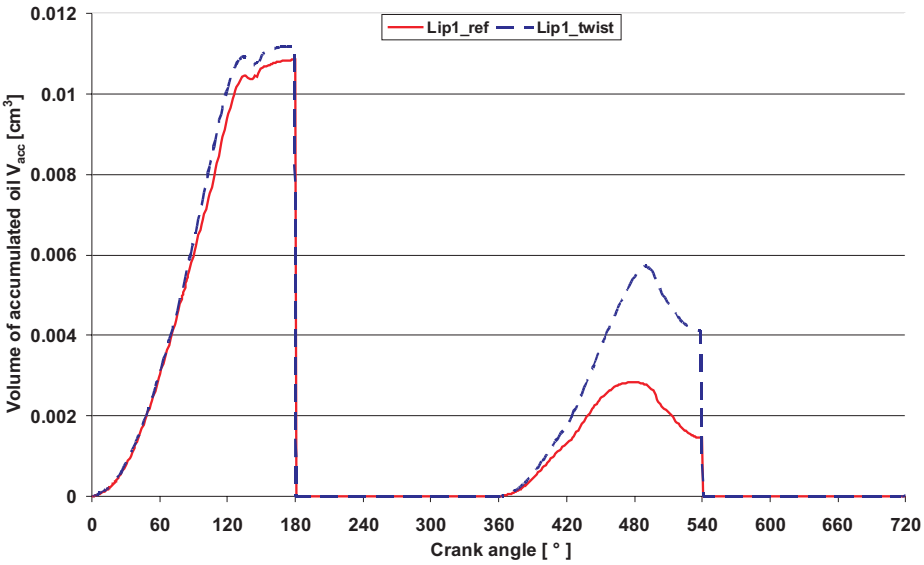

Fig. 19. Comparison of oil volume accumulated by twisting and not twisting compression ring as a function of crankshaft rotation

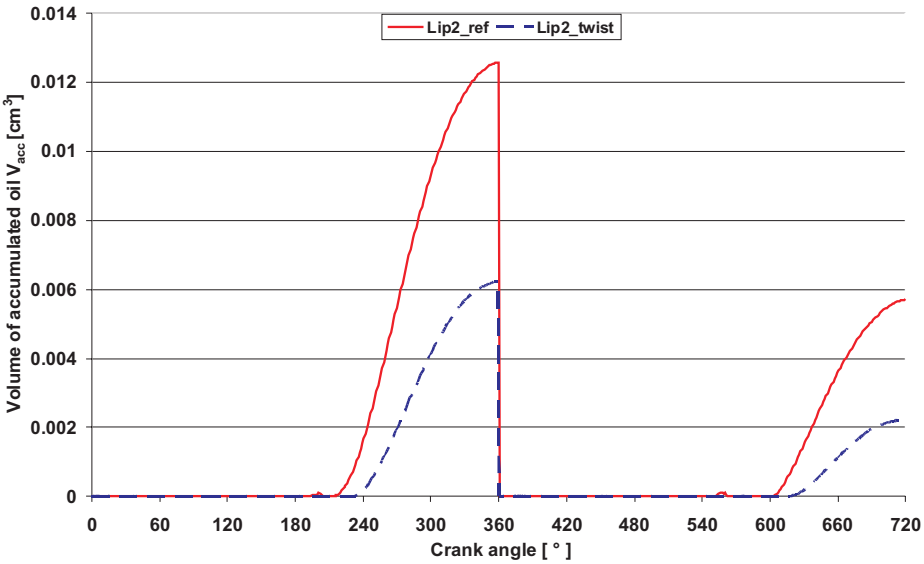

Fig. 20. Comparison of oil volume accumulated by twisting and not twisting a scraper ring as a function of crankshaft rotation

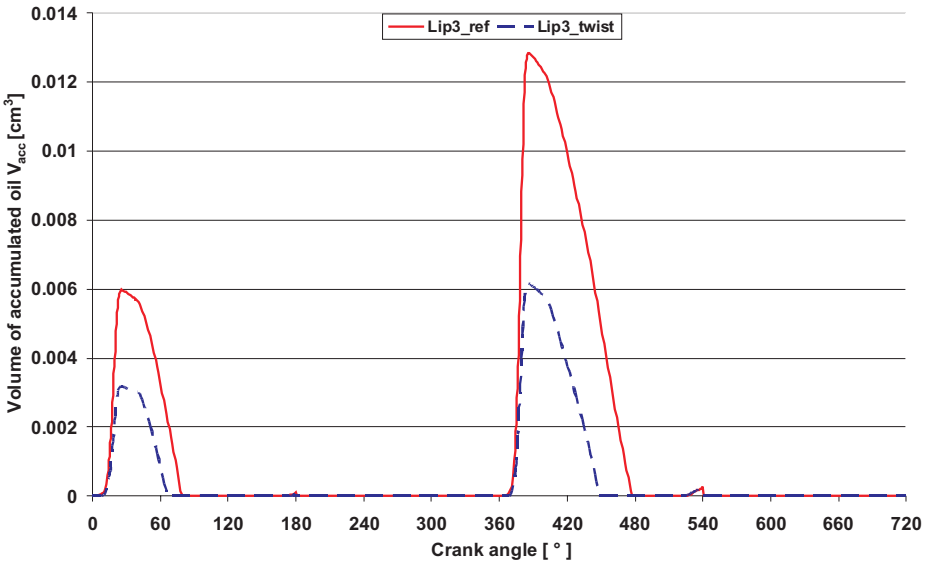

Fig. 21. Comparison of oil volume accumulated by twisting and not twisting of the oil ring upper lip as a function of crankshaft rotation

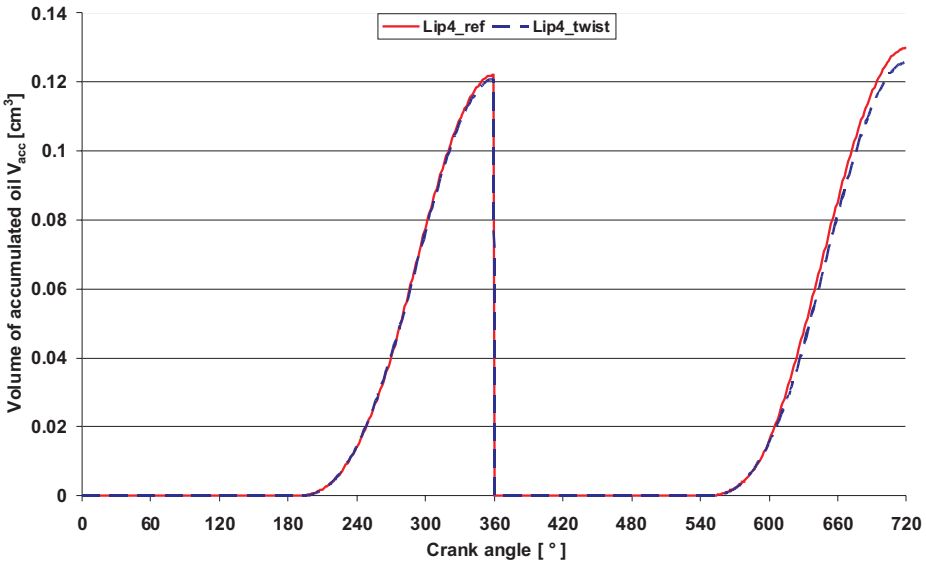

Fig. 22. Comparison of oil volume accumulated by twisting and not twisting of the oil ring lower lip as a function of crankshaft rotation

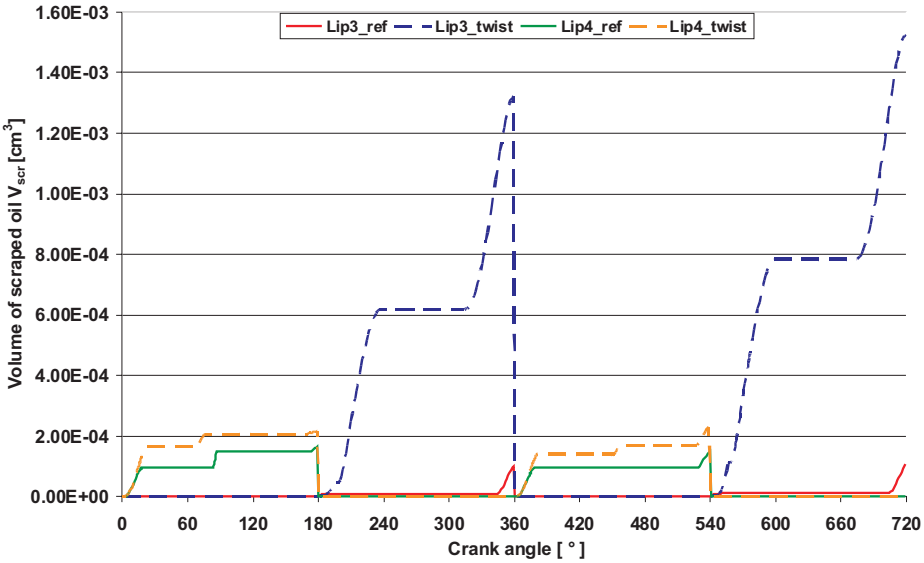

Fig. 23. Comparison of oil volume scraped between lips of a twisting and not twisting oil ring as a function of crankshaft rotation

Fig. 24 depicts changes of the wetted area boundaries on the first (compression) sealing ring. Oil is concentrated on the front part of the ring profile. On the rear part the hydrodynamic pressure drops and this area is ventilated by the gas outside the ring. In the case of very thin oil film, the wetted area is also reduced on the upstream part of the ring surface.

Boundaries of the direct contact of contributing surfaces $\boldsymbol{x_l}$, $\boldsymbol{x_r}$ (see Fig. 2) are depicted (Fig. 24). The contact boundaries have been arbitrarily defined for $h/\sigma = 4$.

Zones of wetting and direct contact for the second (scraper ring) are presented in Fig. 25. Differences in comparison with the first ring result from different ring profiles (see Fig. 9).

Wetted and contact zones for the two-lip third ring are shown in Fig. 26. Characteristic feature of this case is very rapid reduction of the wetted area on the downstream lip. The presented model of a two-lip ring shows the total oil separation of the downstream lip and ventilation of the area in between lips. During the start phase of opposite piston motion, both lips are emerging in the oil film. Again, after a short time the oil separation on the downstream lip is observed. Independent of the direction of motion, the upstream lips are always wetted. One can see short periods of the direct contact of the ring and cylinder liner.

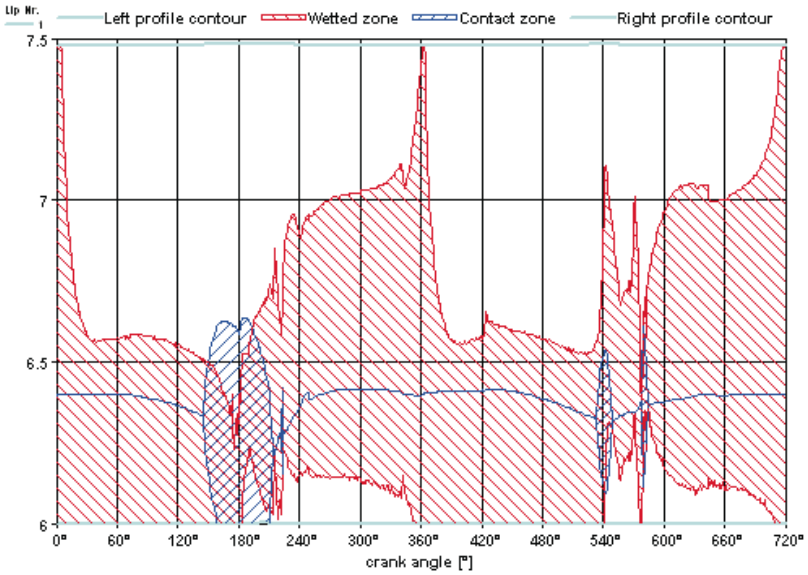

Fig. 24. Oil wetted area and contact zone of the compression ring as a function of crankshaft rotation

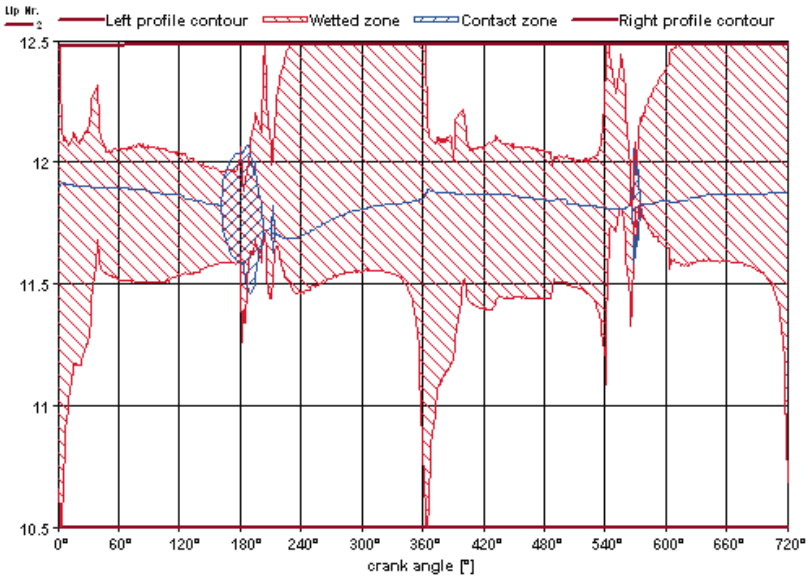

Fig. 25. Oil wetted area and contact zone of the scraper ring as a function of crankshaft rotation

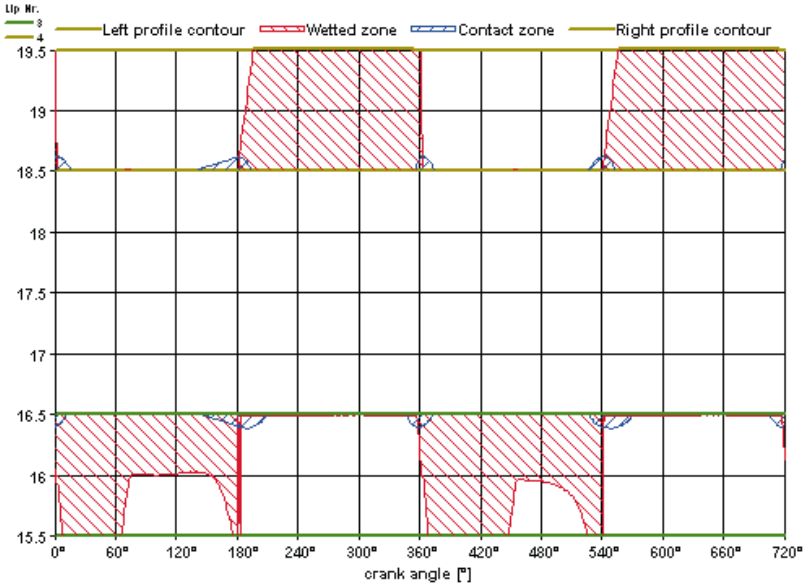

Fig. 26. Oil wetted areas and contact zones of oil ring lands as a function of crankshaft rotation

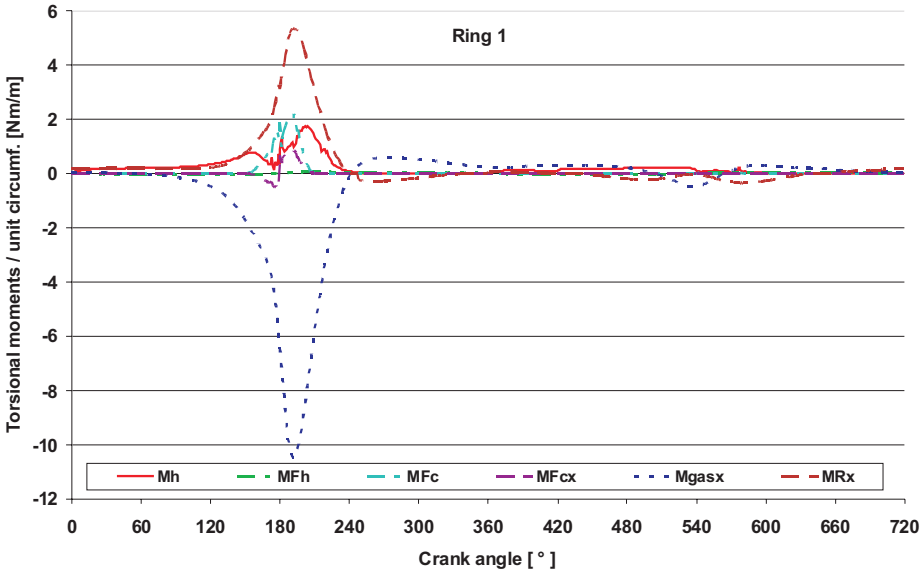

Fig. 27. Variation of torsional moments as a function of crankshaft rotation for the compression ring (M_h – moment of hydrodynamic force, $M_{\mathbf{Fh}}$ – moment of hydrodynamic friction force, $M_{\mathbf{Fc}}$ – moment of radial contact force, $M_{\mathbf{Fcx}}$ – moment of tangential contact force, $M_{textbf\,gasx}$ – moment of gas forces acting on the ring in axial direction, $M_{\mathbf{Rx}}$ – moment of reaction force between the ring and its groove)

The analysis of presented simulation results shows that oil film thickness is very low, and is comparable to the mean value of the coinciding surface roughness in some phases of the piston motion. It suggests the necessity to use the oil flow model proposed by Patir and Cheng [20]. It should be accompanied by the elastic contact model developed by Greenwood and Tripp [6].

The variation of moments proceeded from: gas pressure acting axially $\boldsymbol{M_{gasx}}$, hydrodynamic pressure $\boldsymbol{M_k}$, radial component of the contact force $\boldsymbol{M_{Fc}}$, hydrodynamic friction $\boldsymbol{M_{Fh}}$ and the tangential component of contact force $\boldsymbol{M_{Fcx}}$ was calculated. It can be seen (Fig. 27–29) that the moments: $\boldsymbol{M_{gasx}}$, $\boldsymbol{M_h}$ and $\boldsymbol{M_{Rx}}$ (of the reaction force $\boldsymbol{R_x}$) are the most important. For clearer interpretation of momentum variation, moments have been calculated in relation to the centre of the ring cross-section (point S in Fig 5).

The variation of moments described above is depicted in Fig. 27 for the compression ring, in Fig. 28 for the scraper ring and finally in Fig. 29 for the two lips of the oil ring.

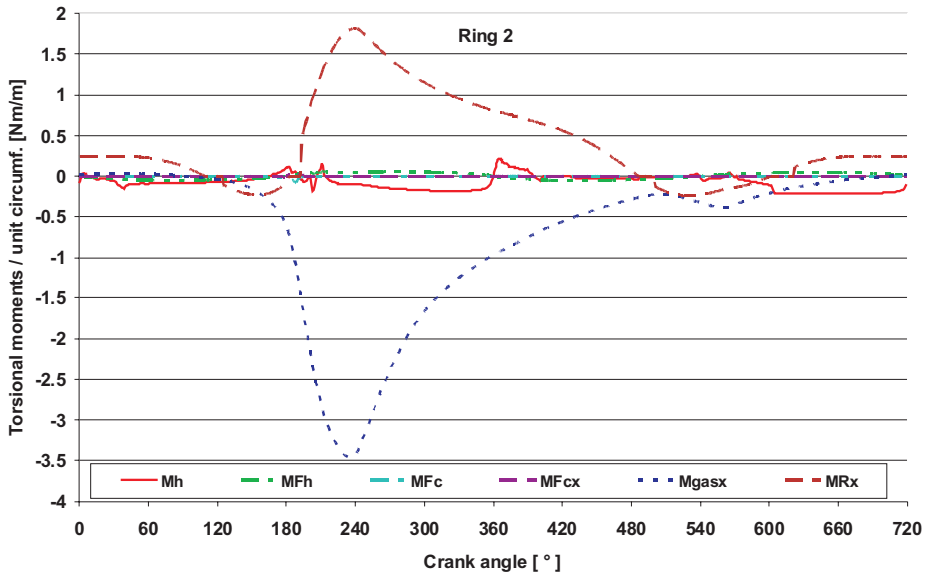

Fig. 28. Variation of torsional moments as a function of crankshaft rotation for the scraper ring (M_h – moment of hydrodynamic force, M_{Fh} – moment of hydrodynamic friction force, M_{Fc} – moment of radial contact force, M_{Fcx} – moment of tangential contact force, M_{gasxh} – moment of gas forces acting on the ring in axial direction, M_{Rx} – moment of reaction force between the ring and its groove)

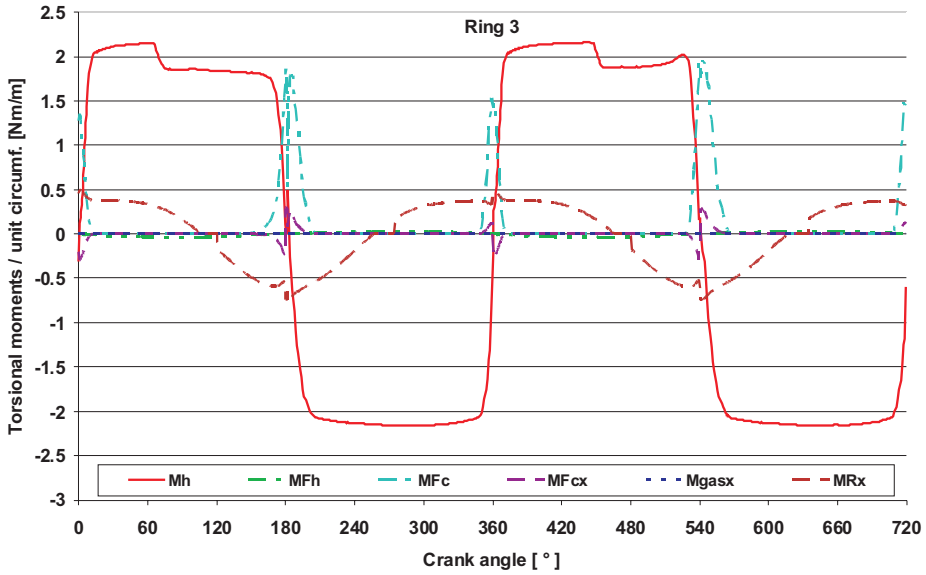

Fig. 29. Variation of torsional moments as a function of crankshaft rotation for the oil ring with two lips (M_h – moment of hydrodynamic force, M_{Fh} – moment of hydrodynamic friction force, M_{Fc} – moment of radial contact force, M_{Fcx} – moment of tangential contact force, M_{gasx} – moment of gas forces acting on the ring in axial direction, M_{Rx} – moment of reaction force between the ring and its groove)

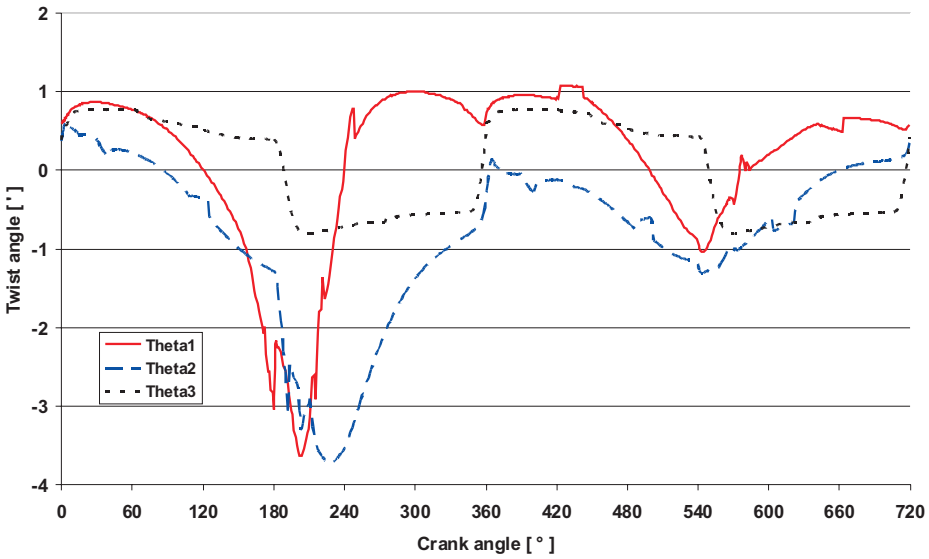

Fig. 30. Variation of twist angles of piston rings as a function of crankshaft rotation (**Theta$_1$** – for the compression ring, **Theta$_2$** – for the scraper ring, **Theta$_3$** – for the oil ring)

Variation of the twist angle for each ring is shown in Fig. 30. Maximal values of the twist angle appear in the phases of piston motion corresponding to high values of gas pressure in the combustion chamber and reach -4'. The ring twists in such a way that the gap deformation causes the decrease of hydrodynamic force and a higher amount of oil scraping is observed.

Variation of the twist angle of the scraper ring is different from that in the compression ring. The twist angle of the compression ring changes its sign, while the scraper ring has mainly the same sign of the twist angle. It should be observed that different twist angles of the considered rings result from different shapes of the scraper and compression ring lips (see Fig. 9).

The twist angle varies between -1' and 1'for the two lip oil ring. Gas forces practically do not influence the oil ring motion. An elastically deformed two lip ring scrapes oil mainly by the consequent lip. The succeeding lip is located deeper in the oil film, scraping oil to the gap between lips. The accumulated oil flows out through the special gaps made in the ring.

6. Conclusions

The main aims of simulation of the ring motion is to predict lubrication conditions, define areas of the possible cylinder liner wear, changes of the piston ring surface shape deformation resulting from wear, and finally to define the gas leakage through the sealing ring set.

Numerical simulation of the ring displacement seems to be an interesting source of information about phenomena associated with the ring operation. Numerical data about ring radial displacement and velocities, data about amounts of scraped oil, oil redistribution, temporary oil film thickness, value of hydrodynamic force, gas force, tangential forces etc. can be collected easily. Collecting such data experimentally is either impossible, or it is very difficult and costly. By analyzing the results of numerical simulations, one can create some theoretical models, or verify the existing ones.

As it has been shown, several problems had to be resolved in order to perform simulation of the ring motion.

Depending on the local value of the ring-liner gap, the oil flow must be described either by the Reynolds equation, or the modified Reynolds equation including coefficients and terms representing the influence of the surface roughness. Both models had to be used alternately for prediction of the hydrodynamic force acting on the ring in the radial direction and friction force acting in the tangent direction. Both models allow us to calculate the hydrodynamic forces using the oil viscosity. The latter was calculated

taking into account mainly oil temperature, local shear stress and local pressure.

When gap values become extremely low, one must include the model of the elastic contact. This model should also predict both (radial and tangent) contact force components.

The radial position of the ring defines the ring stiffness force and ring compensating gap dimension.

It is also necessary to calculate gas pressure in the inter-ring areas. Many investigators have tried to build models and create codes for this purpose.

The authors systematically elaborate the problem of simulation of the piston ring motion, starting from the simple thick oil film model, and improving it by adding the mixed lubrication case, the variation of viscosity due to temperature and pressure and the ring twist mechanism.

For effective modelling of the piston ring motion, it is necessary to simultaneously consider the gas flows through the ring gaps, which define the gas pressure on the back surfaces of rings, and gas forces and oil motion in the ring land – piston liner gap. The influence of the oil film on the gas forces is weak, in contrast to very strong influence of the gas forces on the oil film thickness and lubrication processes.

We have shown the existence of the mixed lubrication process, during which the elements of the ring surface and the liner surface get into a physical contact. This phenomenon has a strong influence on the wear process and deformation of the ring land curvature.

Piston ring can scrape and accumulate some oil volume near the leading edge. This oil is transported to another position on the cylinder liner and redistributed there. This action is strongly influenced by the shape of the ring land, oil film thickness, gas pressure and local piston velocity.

The radial velocity of the ring has an important role in the generation of the hydrodynamic force. If the axial velocity of the piston ring is high enough, the majority of the hydrodynamic force is generated by the variable pressure distribution in the ring and piston liner gap. However, near the piston return points the axial velocity is low, and the only hydrodynamic forces are generated by the squeeze effect in which the radial ring velocity plays an important role.

In some phases of the piston motion, the axial velocity is high enough and oil film thickness so low that the hydrodynamic force equalizing the gas and stiffness forces can be generated only on a part of the ring land. The ring land is then only partially wetted. Definition of the boundaries of the oil film on the ring land is one of the problems which have to be solved.

Rings are located in the piston grooves which have width slightly greater then the width of the ring. This adds additional freedom to the ring motion. The ring can move in the axial direction and can also twist. However, the hydrodynamic force generated in the ring land-cylinder liner is totally compensated by the gas and elastic ring forces. The tangential friction forces acting at some distance from the twist point forms a moment which must be compensated by the stiffness of the twisted ring. Taking into account the presented results of the simulation, one can conclude that the ring twist effect should not be treated as a secondary effect, since relatively low twist angles can cause very significant effects on ring motion behaviour and oil redistribution. Further investigation of these phenomena is strongly recommended.

Manuscript received by Editorial Board, December 21, 2006

REFERENCES

[1] Adams G. G., Müftü S., Azhar N. M.: A Nano-Scale Multi-Asperity Contact and Friction Model, Journal of Tribology, ASME, submitted for review, 2002.
[2] Christensen H.: Some aspects of the functional influence of surface roughness in lubrication, Wear, 17 pp. 149÷162, 1971.
[3] Christensen H.: A theory of mixed lubrication, Proc Instn Mech Engrs, vol. 186, pp. 421÷430, 1972.
[4] Dowson, D., et al.: Piston Ring Lubrication, Part II. Theoretical Analysis of a Single Ring and Complete Ring Pack, Energy Conservation Through Fluid Film Lubrication Technology: Frontiers in Research and Design, ASME Publication, New York, 1979.
[5] Gelinck E.: Mixed Lubrication of Line Contacts, PhD Thesis, University of Twente, 1999.
[6] Greenwood J., Trip J. H.: The contact of Two Nominally Flat Rough Surfaces, Proc IMechE., Vol. 185. pp. 625÷633, 1971.
[7] Gui C. L., Liu K.: Effect of surface roughness on the lubrication properties of the piston ring and cylinder of an engine, and calculation of lubrication and power loss analysis of piston-ring pack of a S195 diesel engine, Lubrication Science 4-4 (4) 263 0954-0075, 1992.
[8] Gulwadi S. D.: Analysis of Tribological Performance of a Piston Ring Pack, Tribology Transaction, Vol. 43, No. 2, pp. 151÷162, 2000.
[9] Iskra A.: Ölverbrauch eines Verbrennungsmotors, Tribologie/Schmierungstechnik 40, Heft 1, pp. 3÷9, 1993.
[10] Jeng Y. R.: Theoretical Analysis of Piston-Ring Lubrication. Part I – Fully Flooded Lubrication. Part II – Starved Lubrication and Its Application to a Complete Ring Pack, Tribology Transactions, Vol. 35, No. 2, pp. 696÷705 and Vol. 4, pp. 707÷714, 1992.
[11] Keribar R., Dursunkaya Z., Flemming M. F.: An Integrated Model of Ring Pack Performance, ASME Transactions, Vol. 113, pp. 382÷389, 1991.
[12] Koszałka G.: Modeling the blowby in internal combustion engine, Part 1: A mathematical model, The Archive of Mechanical Engineering, 2004.
[13] Kozaczewski W.: Konstrukcja grupy tłokowo-cylindrowej silników spalinowych, WKŁ 2004.
[14] Kuo T.-W., Sellnau M. C., Theobald M. A., Jones J. D.: Calculation of Flow in the Piston-Cylinder-Ring Crevices of a Homogenous-Charge Engine and Comparison with Experiment, SAE Paper, No. 890838, 1989.

[15] Liu Q.: Friction in Mixed and Elastohydrodynamic Lubricated Contacts Including Thermal Effects, PhD Thesis, University of Twente, 2002.
[16] Niewczas A.: Trwałość zespołu tłok-pierścienie tłokowe-cylinder silnika spalinowego, WKŁ 1998.
[17] Niewczas A., Koszałka G.: Niezawodność silników spalinowych, Wydawnictwo Uczelniane Politechniki Lubelskiej, Lublin 2003.
[18] Odyck van D. E. A.: Stokes Flow in Thin Films, PhD Thesis, University of Twente, 2001.
[19] Patir N., Cheng H. S.: An Average Flow Model for Determining Effects of Three-Dimensional Roughness on Partial Hydrodynamic Lubrication, Transactions of ASME, Vol. 100, January 1978.
[20] Patir N., Cheng H. S.: Application of Average Flow Model to Lubrication Between Rough Sliding Surfaces, Transactions of ASME, Vol. 101, April 1979.
[21] Rachoor H.: Investigation of dynamic friction in lubricated surfaces, praca doktorska, New Jersey Institute of Technology, 1996.
[22] Radcliffe C. D., Dowson D.: Analysis of Friction in a Modern Automotive Piston Ring Pack, Lubricant and Lubrication/ D. Dowson et al. (editors), Elsevier Science B.V., 1995.
[23] Rangert, B.: Hydrodynamic Piston Ring Lubrication with Reference to Lubricating Oil Consumption, Doctorsavhandlingar vid Chalmers Tekniska, Hogskola, 1974.
[24] Richardson D.E., Borman G.L.: Theoretical and Experimental Investigations of Oil Films for Application to Piston Ring Lubrication, SAE 922341, 1992.
[25] Ruddy B. L., Dowson D., Economous P. N.: A Theoretical Analysis of the Twin-Land Type of Oil-Control Piston Ring, Journal Mechanical Engineering Science, Vol. 23, No. 2, pp. 51÷62, 1981.
[26] Ruddy B. L., Dowson D., Economous P. N.: The Prediction of Gas Pressures within the Ring Packs of Large Bore Diesel Engines, Journal Mechanical Engineering Science, Vol. 23, No. 6, pp. 295÷304, 1981.
[27] Tian T., Wong V. W., Heywood B.: A Piston Ring Pack Film Thickness and Friction Model for Multigrade Oils and Rough Surfaces, SAE Paper, No. 962032, pp. 27÷39, 1996.
[28] Timoshenko S.: Strength of materials, Part II, p. 138, 1962.
[29] Wolff A., Piechna J.: Numeryczna analiza hydrodynamiki układu: pierścienie tłokowe-cylinder silnika spalinowego, Międzynarodowa Konferencja Naukowa: Transport XXI wieku, Warszawa, 19–21.09.2001.
[30] Wolff A., Piechna J.: Numerical simulation of piston ring pack operation, The Archive of Mechanical Engineering, Vol. L, Number 3, pp. 303÷329, 2003.
[31] Wolff A., Piechna J.: Numerical simulation of piston ring pack operation in the case of mixed lubrication, The Archive of Mechanical Engineering, Vol. LII, Number 2, pp. 157÷190, 2005.
[32] Wolff A., Piechna J.: Numeryczna symulacja działania pakietu pierścieni tłokowych, Materiały międzynarodowego kongresu silników spalinowych, referat PTNSS P05-C076, Szczyrk, 25–28.09.2005.
[33] Yun J. E., Chung Y., Chun S. M., Lee K. Y.: An Application of Simplified Average Reynolds Equation for Mixes Lubrication Analysis of Piston Ring Assembly in an Internal Combustion Engine, SAE Paper 952562, 1996.

Numeryczna symulacja działania pakietu pierścieni tłokowych z uwzględnieniem odkształceń kątowych pierścieni

Streszczenie

W artykule przedstawiono model i wyniki symulacji ruchu pakietu pierścieni tłokowych przemieszczających się po filmie olejowym i mogących wykonywać ruchy „kołyszące” w zakresie

ograniczonym wymiarami luzów w rowkach tłoka. W modelu uwzględniono działanie sił hydrodynamicznych, siły elastycznego kontaktu w przypadku częściowego smarowania, siły sprężystości pierścieni, jak też siły gazowe działające na poszczególne pierścienie. Pokazano zmiany momentów skręcających pierścień, zmiany szczeliny smarującej wywołane odkształceniami kątowymi pierścieni i wpływ tych zmian na ruch poszczególnych pierścieni. Wyniki obliczeń przedstawiono w formie wykresów.